A simple ratiometric chemosensor for selective recognition of Cu^{2+} and Hg^{2+} ions from a 100 % aqueous environment

Samadhan R. Patil[a], Jitendra P. Nandre[a], Prashant A. Patil[a], Suban K. Sahoo[b], Manisha Devi[c], Chullikkattil P. Pradeep[c], Yu Fabiao[d], Lingxin Chen[d], Carl Redshaw[e] and Umesh D. Patil*[a]

[a] School of Chemical Sciences, North Maharashtra University, Jalgaon-425001 (M.S.), India,
[b] Department of Applied Chemistry, S.V. National Institute Technology, Surat-395007 (Gujrat), India.
[c] School of Basic Sciences, Indian Institute of Technology Mandi, Himachal Pradesh, 175001, India.
[d] Key Laboratory of Coastal Zone Environmental Processes and Ecological Remediation, Yantai Institute of Coastal Zone Research, Chinese Academy of Sciences, Yantai 264003, China.
[e] Department of Chemistry, University of Hull, Cottingham Road, Hull, HU6 7RX (UK).

Abstract

A simple pyridine based colorimetric receptor 3,3-bis(methylthio)-1-(pyridin-2-yl)prop-2-en-1-one (**BPP**) was synthesized and its cations sensing ability was investigated. During UV-Vis absorption studies, the receptor **BPP** showed an excellent selectivity and sensitivity towards Cu^{2+} and Hg^{2+} over other tested metal cations (Ag^{+}, Al^{3+}, Ba^{2+}, Ca^{2+}, Cd^{2+}, Co^{2+}, Cr^{3+}, Cs^{+}, Fe^{2+}, Fe^{3+}, K^{+}, Li^{+}, Mg^{2+}, Mn^{2+}, Na^{+}, Ni^{2+}, Pb^{2+}, $Sr^{2+}$and Zn^{2+}) with the detection limit down to 1.13 µM (Cu^{2+}) and 1.15 µM (Hg^{2+}). Colorimetrically, the receptor **BPP** showed a selective visual color change from colorless to dark yellow only in the presence of Hg^{2+}. The receptor **BPP** was applied for the detection of Hg^{2+} by test paper strip and supported silica method.

Keywords: Colorimetric chemosensor; Cu^{2+}; Hg^{2+}; 100 % aqueous environment; DFT.

***Corresponding Authors:** Tel: +91-0257-2258431; Fax: +91-0257-2258403 E-mail: mahulikarpp@rediffmail.com (PPM), udpatil.nmu@gmail.com (UDP, former Ass. Prof.).

1. Introduction

The development of new chemosensor for monitoring different analytes, especially heavy and transition metal cations is of pronounced interest because of their importance in chemical, medical, biological and environmental applications [1-3]. Among the various bioactive transition metals, copper is the third most abundant in humans. Copper plays an important role as a catalytic cofactor for a number of metallo-enzymes like superoxide dismutase, cytochrome *c* oxidase, lysyl oxidase, tyrosinase, etc. [4]. However, it's overloading reveals toxicity and a variety of neurological diseases like Alzheimer's, Menken's, Amyotrophic lateral sclerosis, Prion and Wilson's diseases, because of its participation in the formation of reactive oxygen species (ROS) [5-8]. Also, it is an environmental pollutant at high concentrations [9]. Copper, due to its properties like high electrical conductivity, chemical stability, germicidal efficacy and ability to form alloys with other metals [10], has extensively used in the industrial, pharmaceutical and agricultural purposes. Therefore, its widespread use is associated with a serious threat to the environment and living systems [11]. Similarly, chemical sensing of mercury is of equally importance because of its tremendously toxic impact on the environment and biological systems [12-15]. Even though a reduction of its industrial use was observed in the recent years due to strict regulations, but mercury is still present in many products of daily life, such as paints, electronic equipments and batteries [16-17]. Mercury is recognized as a highly poisonous neurological toxin, because of its high affinity for thiol groups in proteins and enzymes, leading to the dysfunction of cells, and consequently causes serious damage to the central nervous and endocrine systems [12-14]. Specially, fetuses and children are very susceptible to the effects of mercury, and even low concentrations of mercury exposure during the early stages of development (by consumption of fish and seafood) can result in a serious neural disorder such as Minamoto disease [18, 19]. These environmental and health problems have prompted the development of analytical methods for the detection and

quantification of mercury as well as copper, especially from the aqueous environment where the conventional techniques are not appropriate.

Currently, a number of methods have been developed to detect Cu^{2+} and Hg^{2+} like inductively coupled plasma detectors, surface plasmon resonance detectors, fluorescence anisotropy assays, quantum dot based assays, electrochemical sensors and fluorescence sensors, atomic absorption spectrometry (AAS), inductively coupled plasma mass spectrometry (ICP-MS), and inductively coupled plasma atomic emission spectrometry (ICP-AES). Although these technologies can detect Cu^{2+} and Hg^{2+} selectively with high sensitivity, but they often require expensive and sophisticated instrumentation, complex sample-preparation steps and highly trained operators are major bottlenecks in their routine applications. On the contrary, the naked-eye detection method allows detection upto micro/submicromolar levels and that too without involving any expensive/sophisticated instruments. Normally, copper and mercury are found as Cu^{2+} and Hg^{2+} in water. Therefore, there is a great demand for the development of highly selective and sensitive colorimetric sensors to detect Cu^{2+} and Hg^{2+} ions from 100 % aqueous environment. However, most of the reported colorimetric sensors for the same purpose by various workers have a number of drawbacks *viz.* poor detection limit, tedious synthetic procedures, use of organic solvents, longer response time, interference from other transition metal ions, and most noticeably the reported sensors are either selective for Cu^{2+} or Hg^{2+} ions only (Table S1) [20-33].

Considering the above facts and as a part of our ongoing research on the design and synthesis of chemosensors [34-37], herein, we have developed a new pyridine based receptor 3,3-bis(methylthio)-1-pyridinyl derivative (**BPP**) (Scheme 1) for the selective detection of Cu^{2+} and Hg^{2+} over other tested nineteen metal cations from 100 % aqueous medium.

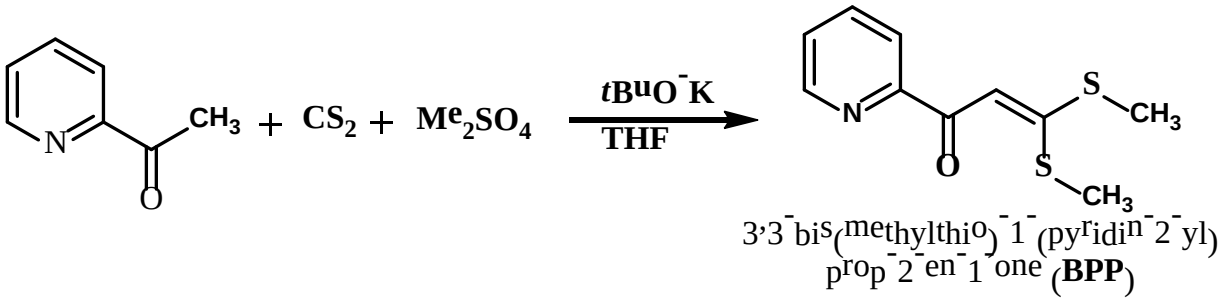

Scheme 1. Synthesis of receptor 3,3-bis(methylthio)-1-(pyridin-2-yl)prop-2-en-1-one (**BPP)**.

2. Experimental

2.1. Materials and Instrumentations

All the starting reagents and metal perchlorates were purchased from either S. D. Fine chemicals or Sigma Aldrich, depending on their availability, and were used as received. All the solvents were of spectroscopic grade and were used without further treatment. The purity of the compounds and the progress of the reactions were determined and monitored by means of analytical thin layer chromatography (TLC). Pre-coated silica gel 60 F_{254} (Merck) on alumina plates (7 x 3 cm) were used and visualized by using a UV-Visible lamp. Melting points were recorded on the Celsius scale by the open capillary method and are uncorrected. IR spectra were recorded on a Perkin-Elmer Spectrum One FT-IR spectrometer as potassium bromide pellets and nujol mulls, unless otherwise mentioned. IR bands are expressed in frequency (cm^{-1}). ^{1}H and ^{13}C NMR spectra were recorded in $CDCl_3$ and DMSO on a 'Jeol ECX-500' Spectrometer, operating at 500 and 125 MHz, respectively, and the chemical shifts are given in ppm downfield from TMS as an internal standard. HR-MS spectra were recorded on a Bruker Impact HD. UV-Vis spectra were recorded on a U-3900 spectrophotometer (Perkine Elmer Co.,USA) with a quartz cuvette (path length=1 cm).

2.2. Spectroscopic Study

The stock solutions of the receptor **BPP** (1.0 x 10^{-3} M, in methanol) and cations (1.0 x 10^{-2} M, in water) were prepared. These solutions were used for all spectroscopic studies after

appropriate dilution. For spectroscopic titrations, the required amount of the diluted solution of receptor **BPP** was taken directly into a cuvette and the spectra were recorded after successive addition of cations by using a micropipette.

*2.3. Synthesis of **BPP***

To a stirred suspension of potassium *tert*-butoxide (9.24 g, 82 mmol) in dry THF (15 mL) at 0 ^{0}C, a solution of 2-acetylpyridine (5 g, 41 mmol) was added through a pressure equalizer funnel, and the mixture was vigorously stirred at 0 ^{0}C for 30 min. Carbon disulphide (3.13 g, 2.5 mL, 41 mmol) was added through a pressure equalizer funnel and the resultant mixture was stirred at 0 ^{0}C for 45 min. The appearance of a reddish solid in the reaction medium indicated the formation of the dipotassium salt of 2-pyridyl-3,3-bissulfanyl-2-propen-1-one. To this suspension, a solution of dimethyl sulphate (10.41 g, 7.8 mL, 82 mmol) in 10 mL dry THF was carefully added drop wise over 10 min whilst maintaining the temperature at 0 ^{0}C. After the addition, the reaction mixture was stirred at 0 ^{0}C for 60 min. On completion of the reaction (TLC; hexane/EtOAc; 8:2), the mixture was transferred into a 250 mL beaker containing 150 g of crushed ice, and the contents of the beaker were thoroughly stirred. A light yellow solid formed, which was filtered and washed with water (50 mL) for three times. The crude solid was recrystallized from 5 % dichloromethane in hexane. Melting point: 106-108 ^{0}C; nature: yellow solid; yield: 46 %; FTIR (KBr, cm^{-1}): 3111-3151 (Py-H), 2996, 2916 (C-H), 1633 (C=C-C=O); ^{1}HNMR (500 MHz, $CDCl_3$, δ ppm): 2.55 (3H, s, -CH_3), 2.62 (3H, s, -CH_3), 7.37-7.39 (1H, m, ArH), 7.63 (1H, s, -CH), 7.79-7.83 (1H, m, ArH), 8.15 (1H, d, *J*=8.25, ArH), 8.62 (1H, d, *J*=4.8, ArH); ^{13}C NMR (125 MHz, $CDCl_3$, δ ppm): 15.02 (-CH_3), 17.41 (-CH_3), 108.75 (-CH), 122.58 (ArC), 125.87 (ArC), 136.91 (ArC), 148.43 (ArC), 154.96 (ArC), 167.72 (CS), 184.32 (C=O); HRMS-m/z: 226.02228 (BPP+H); (Fig. S1, S2, S3 and S4).

2.4. Computational Study

The structural optimization of **BPP** and its host-guest complexes with Cu^{2+} and Hg^{2+} were performed using the computer program Gaussian 09W [38] by applying the density functional theory (DFT) method. All the DFT calculations were performed in the gas phase with a hybrid functional B3LYP (Becke's three parameter hybrid functional using the LYP correlation functional) using the basis sets 6-31G(d,p) for C, H, N, S atoms and LANL2DZ for Cu, Hg atoms.

3. Results and discussion

The receptor **BPP** was synthesized by the known literature procedure as depicted in Scheme 1 [39]. The metal ion recognition capability of the pyridine based receptor 3,3-bis(methylthio)-1-(pyridin-2-yl)prop-2-en-1-one (**BPP**) was explored by using simple, sensitive and inexpensive analytical techniques such as UV-Vis absorption spectroscopy, ^{1}H NMR spectroscopy and by naked-eye detection.

3.1. Naked-eye experiment

In the naked-eye experiment, two equivalents of different metal ions (40 µL, 1 x 10^{-2} M, Cu^{2+}, Hg^{2+}, Ag^{+}, Al^{3+}, Ba^{2+}, Ca^{2+}, Cd^{2+}, Co^{2+}, Cr^{3+}, Cs^{+}, Fe^{2+}, Fe^{3+}, K^{+}, Li^{+}, Mg^{2+}, Mn^{2+}, Na^{+}, Ni^{2+}, Pb^{2+}, Sr^{2+} and Zn^{2+}) were separately added to the receptor **BPP** solution [2 mL, 1 x 10^{-4} M, methanol:water (30:70, v/v)]. As shown in Fig. 1, a distinct color change from colorless to a dark yellow color was observed only in the presence of Hg^{2+} ions. No significant color changes were observed with the other tested metal ions including Cu^{2+}, which clearly revealed that the receptor **BPP** can be used for the 'naked-eye' detection of Hg^{2+} ions in aqueous medium. Furthermore, a study on the naked-eye detection limit for Hg^{2+} (1 x 10^{-2} to 1 x 10^{-5} M, Fig. S5) by the receptor **BPP** inferred that this receptor can be used to detect Hg^{2+} down to 1 x 10^{-4} M levels.

Fig. 1. Photograph of the vials containing **BPP** [2 mL, 1 x 10^{-4} M, methanol:water (30:70, v/v)] in the presence of the different tested metal cations (40 µL, 1 x 10^{-2} M, in water).

*3.2. UV-Vis studies of **BPP** with cations*

After the naked-eye results, we moved towards the systematic study of chemosensing behavior of **BPP** by UV-Vis spectroscopy. All spectroscopic measurements of receptor **BPP** (7.5 x 10^{-5} M) were performed in methanol:water (30:70, v/v) solution. The receptor **BPP** exhibited three absorption bands at 249 nm, 282 nm and 349 nm (Fig. 2). The absorption spectrum of **BPP** showed changes selectively only upon the addition of five equivalents of Cu^{2+} and Hg^{2+} ions (75 µL each, 1 x 10^{-2} M, in water). With Cu^{2+}, the receptor exhibited a broad absorption band with maxima at 410 nm. In contrast, upon the addition of Hg^{2+} ions, a new red-shifted charge transfer band was appeared at 450 nm (Fig. 2). The appearance of the red shifted band at ~ 450 nm was responsible for the observed remarkable color change of **BPP** with Hg^{2+} ions. No noticeable changes in the absorption profile of **BPP** were observed with other tested cations, which clearly indicate the selective recognition ability towards Cu^{2+} and Hg^{2+} ions. Also, the observed spectral changes of **BPP** at different wavelengths (410 and 450 nm) can be used to detect and discriminate the presence of both Cu^{2+} and Hg^{2+} ions.

Fig. 2. UV-Vis absorption spectra of receptor **BPP** [2 mL, 7.5 x 10^{-5} M, methanol:water (30:70, v/v)] in the presence of five equivalents of different tested metal cations (75 µL, 1 x 10^{-2} M, in water).

To gain more insights into the cations chemosensing ability and mechanism of **BPP**, the absorption titrations were performed with Cu^{2+} and Hg^{2+} ions. As shown in Fig. 3, upon incremental addition of Cu^{2+} ions (0-300 µL, 1 x 10^{-3} M, in water), the intensity of absorption band centered at 410 nm was continuously increased with the formation of an isosbestic point at 242 nm. Similarly, upon successive addition of Hg^{2+} ions (0-300 µL, 1 x 10^{-3} M, in water), the absorption band of **BPP** at 349 nm was markedly decreased with the concomitant appearance of the new broad peak between 400-500 nm (Fig. 4). Also, two distinct isosbestic points at 244 nm

and 400 nm were observed, which clearly delineated the formation of equilibrium between the receptor **BPP** and **BPP.**Hg^{2+} complex.

Fig. 3. UV-Vis absorption titration spectra of **BPP** (7.5 x 10^{-5} M) in methanol:H_2O (30:70) with the addition of 0-2 equivalents of Cu^{2+} ions (0-300 µL, 1 x 10^{-3} M, in H_2O).

Fig. 4. UV-Vis absorption titration spectra of **BPP** (7.5 x 10^{-5} M) in methanol:H_2O (30:70) with the addition of 0-2 equivalents of Hg^{2+} ions (0-300 µL, 1 x 10^{-3} M, in H_2O).

From the absorption titration data, a linear dependence of absorption at 410 nm/450 nm was observed as a function of Cu^{2+}/Hg^{2+} concentrations (Fig. S6-7), and thereby the stoichiometry of **BPP** with Cu^{2+}/Hg^{2+} could be estimated to be 1:1. Moreover, the mole ratio plot (Fig. S8-9) and the Job's plot (Fig. S10-11) support the formation of a complex between **BPP** and Cu^{2+}/Hg^{2+} in 1:1 binding stoichiometry. Further, a more direct evidence for the formation of 1:1 complex was obtained from the ESI-MS spectra of **BPP** in the presence of 1.0 equivalent Cu^{2+}/Hg^{2+} in methanol/water (30:70, *v/v*) (Fig. S12-13). The main characteristic MS peak was observed at *m/z* = 226.02228 ([**BPP**+H]$^+$) for pure **BPP** (Fig. S2). However, on addition of 1.0 equivalent of Cu^{2+}, the peak at 226.02228 was disappeared and a new peak appeared at *m/z* = 361.7721 corresponding to the complex [**BPP.**Cu.$(H_2O)_2$+K–H] (Fig. S12). Similarly, ESI-MS analysis data of **BPP** in the presence of 1.0 equivalents Hg^{2+} showed a peak at *m/z* = 477.9179 corresponding to the complex [**BPP.**Hg.H_2O+K] (Fig. S13).

Based on the 1:1 stoichiometry for **BPP**.Cu^{2+} complexation, the binding constant (*K*a) of **BPP** with Cu^{2+}/Hg^{2+} was determined using Benesi-Hilderbrand plot analysis, by using the following equation (1).

$$\frac{1}{A - A_0} = \frac{1}{Ka(A_{max} - A_0)[Cu(II)]} + \frac{1}{A_{max} - A_0} \qquad (1)$$

Where, A and A_0 are the absorbance of **BPP** solution in the presence and absence of Cu^{2+}/Hg^{2+}, respectively; A_{max} is the saturated absorbance of **BPP** in the presence of excess amounts of Cu^{2+}/Hg^{2+} and [Cu^{2+}/Hg^{2+}] is the concentration of Cu^{2+}/Hg^{2+} ions added (mol L^{-1}). Plotting of 1 / (ΔA) vs 1 / [Cu^{2+}/Hg^{2+}] showed a linear relationship (Fig. 5 and 6), which also suggests that **BPP** bounds with Cu^{2+}/Hg^{2+} in a 1:1 stoichiometry. The binding constant (*K*a) was determined from the slope and found to be 13,380 M^{-1} and 4,496 M^{-1} for the **BPP**.Cu^{2+} and **BPP**.Hg^{2+} complex, respectively.

The limit of detection (LOD) and limit of quantification (LOQ) of the receptor **BPP** was next calculated. According to the IUPAC definition, the LOD and LOQ was calculated using the relationship LOD = (3.3 x standard deviation)/slop and LOQ = (10 x standard deviation)/slop. To calculate the relative standard deviation, the absorption measurements of ten blank samples were recorded. The calibration curves (absorbance *vs* [Cu^{2+}/Hg^{2+}]) were plotted (Fig. S6 & S7), and then the obtained slope was used to calculate the LOD and LOQ. The obtained LOD value for Cu^{2+} ions was 1.13 µM and 1.15 µM for Hg^{2+} ions, whereas the LOQ value for Cu^{2+} ions was 3.42 µM and 3.45 µM for Hg^{2+} ions.

Fig. 5. Benesi-Hildebrand plot of 1/ [ΔA] against 1 / [Cu^{2+}].

Fig. 6. Benesi-Hildebrand plot of 1/ [ΔA] against 1 / [Hg^{2+}].

3.3. Possible sensing mechanism

The proposed binding modes and the computed molecular structure of **BPP** and its **BPP.**Hg^{2+}/Cu^{2+} complex was shown in Fig. 7. The receptor **BPP** has multiple donor sites to make complex with Hg^{2+}/Cu^{2+}. Therefore, different possible binding modes were tested in the theoretical calculations. Based on the calculated energy, the carbonyl-O and pyridine-N atoms of the receptor **BPP** take part in forming a stable complex with Hg^{2+}/Cu^{2+}. On complexation of

BPP with Hg^{2+} and Cu^{2+} resulted in the lowering of interaction energy ($E_{int} = E_{complex}-E_{receptor}-E_{Hg^{2+}/Cu^{2+}}$) by -248.45 kcal/mol and -345.08 kcal/mol respectively, which indicates the formation of a stable complex. Further, the frontier molecular orbitals (FMOs) plots (Fig. 8) of **BPP** and its **BPP**.Hg^{2+}/Cu^{2+} complexes was next analyzed which indicates the intramolecular charge transfer (ICT) occurred between the receptor and metal ions (Hg^{2+}/Cu^{2+}). Also, the band gap between the highest occupied molecular orbital (HOMO) and lowest unoccupied molecular orbital (LUMO) of **BPP** was lowered on complexation with Hg^{2+}/Cu^{2+}. The DFT results corroborate well with the shift in the absorption band of **BPP** on complexation with Hg^{2+}due to ICT process.

In addition, the complexation mode was verified by performing the ^{1}H NMR titrations of **BPP** by adding various equivalents of Hg^{2+} in DMSO-d_6. On addition of 1 equivalent of Hg^{2+}, the peaks due to aromatic protons showed a downfield shift from δ 8.62, 8.15 and 7.83 to δ 9.36, 8.75 and 8.32 and get broden (Fig. S14). This is probably due to the complexation of Hg^{2+} with nitrogen [40]. Simultaneously, the -CH proton exhibited an upfield shift from δ 7.58 to 6.89, probably due to the delocalization of electrons as shown in Fig. 8. Further, we also carried out ^{1}H NMR titration experiments on **BPP** in $CDCl_3$ solutions with the addition of various equivalents of the copper perchlorate. Peak broadening was observed on addition of copper perchlorate to **BPP** (Fig. S15), probably due to the paramagnetic nature of copper.

Fig. 7. The DFT computed structure of **BPP** and its complexes Hg^{2+} and Cu^{2+}.

Fig. 8. The DFT computed LUMO (above) and HOMO (below) diagrams of (a) **BPP**, (b) **BPP**.Hg^{2+}, (c) **BPP**.Cu^{2+} (alpha MO's) and **BPP**.Cu^{2+} (beta MO's).

*3.4. Practical applications of **BPP***

The UV-Vis responses of the receptor **BPP** to various possible interfering metal ions and its selectivity for Cu^{2+} and Hg^{2+} ions were tested (Fig. S16 & S17). For this study, two equivalents of Cu^{2+} and Hg^{2+} ions were added to the solution containing **BPP** and the other competitive metal ions (two equivalents) of interest; and their absorption spectra were recorded. From the obtained data, we observed that the sensing of both Cu^{2+} and Hg^{2+} by chemosensor **BPP** was found to be hardly affected by the commonly co-existent miscellaneous competitive cations. Importantly, the colorimetric and spectral responses of **BPP** towards of Hg^{2+} were not interfered even in the presence of Cu^{2+}.

Therefore, in order to ensure that **BPP** is potentially of practical use, **BPP** loaded test strips were prepared to detect Hg^{2+}. The desired test strips were prepared by soaking small strip of cellulose paper (Whatman No. 42) in the solution of **BPP** ($1x10^{-2}$ M) in methanol and then dried in air. When this strip was treated with 10 mL aqueous solution of Hg^{2+} ($1x10^{-4}$ M), the colorless strip sharply turned into dark yellow color (Fig. 9 and supporting video). The rapid color change of the test strip in solution clearly inferred the practical application of **BPP** for the qualitative detection of Hg^{2+} in aqueous medium.

Fig. 9. Practical application of **BPP** for the detection of Hg^{2+} by test strip method.

The sensing of Hg^{2+} by **BPP** also worked on a solid support (Fig. 10). The silica gel (60-120 mesh, 5.0 g, colorless) was soaked in **BPP** (in methanol, 5 mL, $1x10^{-2}$ M) and then the solvent was removed. A faint greenish color of the silica gel was appeared which indicates the adsorption of the receptor on the surface. When it was treated with 10 mL aqueous solution of Hg^{2+} ($1x10^{-4}$ M), the colorless solution promptly turned to a dark yellow color (supporting video). The instantaneous color change of the solid silica gel in solution clearly inferred the practical application of **BPP** for the qualitative detection of Hg^{2+} in aqueous medium.

Fig. 10. Practical application of **BPP** for detection of Hg^{2+} by silica support method.

4. Conclusion

In conclusion, we have developed a simple yet highly selective and sensitive chemosensor **BPP** for the detection of Cu^{2+} and Hg^{2+} ions. The red-shift to 450 nm and dramatic enhancement at 410 nm in the absorbance of **BPP** solution [methanol:water (30:70)] was observed in the presence of Hg^{2+} and Cu^{2+} ions, respectively. The chemosensor **BPP** displays a high specificity for Cu^{2+} and Hg^{2+} ions without or with little interference from other tested ions. The remarkable spectral sensing of **BPP** confirmed a 1:1 (**BPP**.Cu^{2+}/Hg^{2+}) binding model with the detection limit down to micromolar range. Importantly, the recognition of Hg^{2+} was also confirmed by the remarkable color change of **BPP** from colorless to dark yellow color. In addition, the receptor **BPP** was applied to detect Hg^{2+} in the aqueous media by naked-eye using test strip and silica support methods.

Acknowledgement

The author Dr. U. D. Patil is grateful for the financial support from the Department of Science& Technology, New Delhi, India (Reg. No. CS-088/2013). R. S. Patil thanks UGC, New Delhi for the award of RFSMS fellowship and financial support.

Appendix A. Supplementary data

Supplementary data associated with this article can be found, in the online version, at doi:0000000..2014...

References

1 V. Amendola, L. Fabbrizzi, M. Licchelli, C. Mangano, P. Pallavicini, L. Parodi, A. Poggi, Coord. Chem. Rev. 190-192 (1999) 649-669.

2 K. Rurack, Spectrochim. Acta A Mol. Biomol. Spectrosc. 57 (2001) 2161-2195.

3 L. Prodi, F. Bolletta, M. Montalti, N. Zaccheroni, Coord. Chem. Rev. 205 (2000) 59-83.

4 K.D. Karlin, Science 261 (1993) 701-708.

5 R.A. Løvstad, Biometals 17 (2004) 111-113.

6 D. Strausak, J.F.B. Mercer, H.H. Dieter, W. Stremmel, G. Multhaup, Brain Res. Bull. 55 (2001) 175-185.

7 E. Gaggelli, H. Kozlowski, D. Valensin, G. Valensin, Chem. Rev. 106 (2006) 1995-2044.

8 Metal Ions in Biological Systems, Properties of Copper; Vol. 12; Sigel, H., Ed.; Dekker: New York, 1981.

9 L. Tapia, M. Suazo, C. Hodar, V. Cambiazo, M. Gonzalez, Biometals 16 (2003) 169-174.

10 A.K. Jain, R.K. Singh, S. Jain, J. Raisoni, Transition Met. Chem. 33 (2008) 243-249.

11 S.L. Belli, A. Zirino, Anal. Chem. 65 (1993) 2583-2589.

12 H.R. Sunshine, S.J. Lippard, Nucleic Acids Res. 1 (1974) 673-688.

13 J.W. Sekowski, L.H. Malkas, Y.T. Wei, R.J. Hickey, Toxicol. Appl. Pharmacol. 145 (1997) 268-276.

14 I. Onyido, A.R. Norris, E. Buncel, Chem. Rev. 104 (2004) 5911-5929.

15. W.F. Fitzgerald, C.H. Lamborg, C.R. Hammerschmidt, Chem. Rev. 107 (2007) 641-662.

16. Q.R. Wang, D. Kim, D.D. Dionysiou, G.A. Sorial, D. Timberlake, Environ. Pollut. 131 (2004) 323-336.

17. T.W. Clarkson, L. Magos, G.J. Myers, Engl. J. Med. 349 (2003) 1731-1737.

18. F. Zahir, S.J. Rizwi, S.K. Haq, R.H. Khan, Environ. Toxicol. Pharmacol. 20 (2005) 351-360.

19. J.G. Dorea, C.M. Donangelo, Clin. Nutr. 25 (2006) 369-376.

20. Z.-C. Wen, R. Yang, H. He, Y.-B. Jiang, Chem. Commum. (2006) 106-108.

21. W. Lin, L. Yuan, W. Tan, J. Feng, L. Long, Chem. Eur. J. 15 (2009) 1030-1035.

22. P. Xie, F. Guo, C. Li, Y. Xiao, Can. J. Chem. 89 (2011) 1364-1369.

23. A. Kumar, V. Kumar, U. Diwan, K.K. Upadhyay, Sens. Actuators, B 176 (2013) 420-427.

24. D. Maity, A.K. Manna, D. Karthigeyan, T.K. Kundu, S.K. Pati, T. Govindraju, Chem. Eur. J. 17 (2011) 11152-11161.

25. Q. Li., M. Peng, N. Li, J. Qin, Z. Li., Sens. Actuators, B 173 (2012) 580-584.

26. H.M. Chawla, P. Geol, R. Shukla, Tetrahedron Lett. 55 (2014) 2173-2176.

27. A. Thakur, S. Sardar, S. Ghosh, Inorg. Chem. 50 (2011) 7066-7073.

28. V. Bhalla, R. Tejpal, M. Kumar, A. Sethi, Inorg. Chem. 48 (2009) 11677-11684.

29. M. Alfonso, J. Contreras-Garcia, A. Espinosa, A. Tarraga, P. Molina, Dalton Trans. 41 (2012) 4437-4444.

30. V. Bhalla, Roopa, M. Kumar, P.R. Sharma, T. Kaur, Inorg. Chem. 51 (2012) 2150-2156.

31. S. Tang, P. Tong, W. Lu, J. Chen, Z. Yan, L. Zhang, Biosens. Bioelectron. 59 (2014) 1-5.

32. Q. Lin, Y.-P. Fu, P. Chen, T.-B. Wei, Y.-M. Zhang, Dyes Pigments 96 (2013) 1-6.

33. D. Udhayakumari, S. Velmathi, J. Lumin. 136 (2013) 117-121.

34. J.P. Nandre, S.R. Patil, V.S. Patil, F. Yu, L. Chen, S.K. Sahoo, T. Prior, C. Redshaw, P.P. Mahulikar, U.D. Patil, Biosens. Bioelectron. 61 (2014) 612-617.

35. D. Sharma, S.K. Sahoo, S. Chaudhary, R.K. Bera, J.F. Callan, Analyst 138 (2013) 3646-3650.

36. S.R. Patil, J.P. Nandre, D. Jadhav, S. Bothra, S.K. Sahoo, M. Devi, C.P. Pradeep, P.P. Mahulikar, U.D. Patil, Dalton Trans. (2014) DOI: 10.1039/C4DT01516A.

37. A.K. Gupta, A. Dhir, C.P. Pradeep, Dalton Trans. 42 (2013) 12819-12823.

38. H.B. Schlegel, G.E. Scuseria, M.A. Robb, J.R. Cheeseman, G. Scalmani, V. Barone, B. Mennucci, G.A. Petersson, H. Nakatsuji, M. Caricato, X. Li, H.P. Hratchian, A.F. Izmaylov, J. Bloino, G. Zheng, J.L. Sonnenberg, M. Hada, M. Ehara, K. Toyota, R. Fukuda, J.

Hasegawa, M. Ishida, T. Nakajima, Y. Honda, O. Kitao, H. Nakai, T. Vreven, J.A. Montgomery, Jr., J.E. Peralta, F. Ogliaro, M. Bearpark, J.J. Heyd, E. Brothers, K.N. Kudin, V.N. Staroverov, R. Kobayashi, J. Normand, K. Raghavachari, A. Rendell, J.C. Burant, S.S. Iyengar, J. Tomasi, M. Cossi, N. Rega, J.M. Millam, M. Klene, J.E. Knox, J.B. Cross, V. Bakken, C. Adamo, J. Jaramillo, R. Gomperts, R.E. Stratmann, O. Yazyev, A.J. Austin, R. Cammi, C. Pomelli, J.W. Ochterski, R.L. Martin, K. Morokuma, V.G. Zakrzewski, G.A. Voth, P. Salvador, J.J. Dannenberg, S. Dapprich, A.D. Daniels, Ö. Farkas, J.B. Foresman, J. V. Ortiz, J. Cioslowski, D.J. Fox, Gaussian 09, Revision A.1, Gaussian, Inc., Wallingford CT (2009).

39. H.S.P. Rao, S. Sivakumar. J. Org. Chem. 71 (2006) 8715-8723.

40. J. Wang, X. Qian, J. Cui, J. Org. Chem. 71 (2006) 4308-4311.